Metamagnetic transition and magnetic phase diagram in $NaZn_{13}$-type $Pr_{0.2}La_{0.8}Fe_{11.4}Al_{1.6}$ compound

Jing Chen
State Key Laboratory for Magnetism, Institute of Physics, Chinese Academy of Science, Beijing 100080, China and Department of Applied Physics, Wuhan University of Science and Technology, Wuhan 430081, China

Hong-wei Zhang[a)]
State Key Laboratory for Magnetism, Institute of Physics, Chinese Academy of Science, Beijing 100080, China

Li-gang Zhang
Department of Applied Physics, Wuhan University of Science and Technology, Wuhan 430081, China

Ji-rong Sun and Bao-gen Shen
State Key Laboratory for Magnetism, Institute of Physics, Chinese Academy of Science, Beijing 100080, China

(Received 7 October 2007; accepted 8 October 2007; published online 4 December 2007)

Antiferromagnetic (AFM) state with the Néel temperature around 190 K is observed in $NaZn_{13}$-type $Pr_{0.2}La_{0.8}Fe_{11.4}Al_{1.6}$ compound, similar to that in $LaFe_{11.4}Al_{1.6}$. After a zero-field-cooling process, a ferromagnetic (FM) state is induced at ~70 K by applying a magnetic field no less than 0.4 T for $Pr_{0.2}La_{0.8}Fe_{11.4}Al_{1.6}$. The AFM-to-FM transition is irreversible at low temperature, but reversible at high temperature. A partial reversible behavior is found at temperature ranging from 70 to 85 K. A magnetic phase diagram is made based on the magnetic measurement. To explain the peculiar diagram, a phenomenological model is proposed. The model is based on a combination of itinerant electronic metamagnetism and the theory for thermal activation. © *2007 American Institute of Physics*. [DOI: 10.1063/1.2819368]

INTRODUCTION

$LaFe_{13-x}Al_x$ ($1.04 \leqslant x \leqslant 7.02$) compounds with a cubic $NaZn_{13}$-type structure have drawn considerable attention due to their multiple magnetic states.[1–11] Mictomagnetic, ferromagnetic, and antiferromagnetic regimes are observed sequentially with increasing iron concentration. A long-range-ordered antiferromagnetic state, consisting of ferromagnetic clusters coupled antiferromagnetically, is confirmed in the compounds with $x=1.17$ via neutron scattering at 4.2 K.[11] With the help of Mössbauer spectroscopy, it is revealed that $LaFe_{13-x}Al_x$ compounds with $1.04 \leqslant x \leqslant 1.69$ present an antiferromagnetic (AFM) state.[9,11] The appearance of AFM is related to the short Fe-Fe interatomic distances. For ferromagnetic $LaFe_{13-x}Al_x$ with $x=1.82$, the transition from the ferromagnetic (FM) state to AFM state can be induced by a high pressure,[4] which verifies the Fe-Fe distance dependent magnetism. In the concentration range of $1.04 \leqslant x \leqslant 1.69$, AFM state may be instable due to such a closely packed structure. Changes in the magnetic ground state can be caused by the application of magnetic field,[2,3] pressure,[4] thermal excitation,[5] or insertion of interstitial atoms,[6–8] which leads to the discoveries of large magnetovolume, magnetoresistance, and magnetocaloric effects near the temperature for phase transition.[2,8–10]

Recently, a peculiar magnetic phase diagram, similar to that intensively debated in the Gd_5Ge_4 compound,[12–16] is found in $LaFe_{11.4}Al_{1.6}$ with very low interstitial carbon content.[17] It is easy to understand that a FM state can be induced by the enlargement of the Fe-Fe distance after introducing the interstitial atoms into $LaFe_{11.4}Al_{1.6}$.[6–8,17] However, the reason why such peculiar magnetic phase diagrams appear is still unknown.[17] In this work, the effect of substituting Pr for La on the magnetic properties of the parent $LaFe_{11.4}Al_{1.6}$ compound has been investigated. The substitution first leads to the introduction of the Pr-Pr intrasublattice and the Pr-Fe intersublattice ferromagnetic exchange interactions, and then affects the antiferromagnetism in the parent alloy. Unexpectedly, the peculiar magnetic phase diagram is also obtained in the $Pr_{0.2}La_{0.8}Fe_{11.4}Al_{1.6}$ compound. It is clear that the Gd_5Ge_4 compound belongs to a localized moment system with a layered crystal structure, and the observed complex magnetic transformation has a close relationship with the exchange interactions between and within the slabs. However, the $Pr_{0.2}La_{0.8}Fe_{11.4}Al_{1.6}$ compound is of typical itinerant-electron system.[1–9] Furthermore, although the peculiar magnetic phase diagram in $Pr_{0.2}La_{0.8}Fe_{11.4}Al_{1.6}$ is similar to that in $LaFe_{11.4}Al_{1.6}C_{0.02}$,[17] the cause may be different because of the following reason. The crystal lattice is contracted by the substitution of Pr for La due to the well-known lanthanide contraction, whereas the lattice is enlarged by introducing the interstitial carbon into the parent alloy $LaFe_{11.4}Al_{1.6}$. Therefore, it is meaningful to explore the nature of the magnetic phase diagram in $Pr_{0.2}La_{0.8}Fe_{11.4}Al_{1.6}$.

[a)]Author to whom correspondence should be addressed. Electronic mail: hwzhang@g203.iphy.ac.cn.

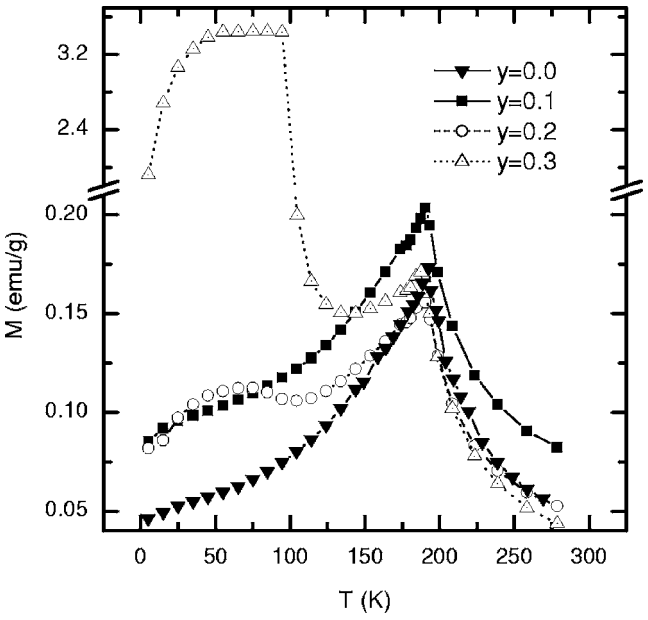

FIG. 1. ZFC isofield magnetization curves under the field of 0.01 T for $Pr_yLa_{1-y}Fe_{11.4}Al_{1.6}$ compound with $y=0$, 0.1, 0.2, and 0.3.

EXPERIMENT

$Pr_yLa_{1-y}Fe_{11.4}Al_{1.6}$ compound was prepared by arc melting in argon atmosphere with purities of the elements higher than 99.9%. The ingots were vacuum annealed at 1223 K for 13 days. $LaFe_{11.4}Al_{1.6}$ compound was also prepared for comparison. A nearly single $NaZn_{13}$-type phase in the samples with $y<0.4$ is verified by x-ray powder diffraction measurements. Magnetic measurements were performed on a commercial MPMS-7 superconducting quantum interference device magnetometer. The isofield magnetization $M(T)$ curves were obtained by warming up the samples with two modes, zero-field cooling (ZFC) and field cooling (FC). In the ZFC (FC) mode, the sample is cooled from 200 to 5 K before (after) the measuring field is switched on.

RESULTS AND DISCUSSION

Figure 1 shows the ZFC $M(T)$ curves for $Pr_yLa_{1-y}Fe_{11.4}Al_{1.6}$ samples under the field of $\mu_0H=0.01$ T. The cusps at 188–193 K indicate the occurrence of the AFM-to-PM transition (PM denotes paramagnetic). The Néel temperature for $LaFe_{11.4}Al_{1.6}$ is the same as that reported in Ref. 1. However, compared with the $LaFe_{11.4}Al_{1.6}$ compound, there is a broadened cusp around 70 K in the sample with $y=0.2$. Furthermore, at the temperature ranging from 50 to 100 K, a FM state is evidently observed in the sample with $y=0.3$. Therefore, we focus on the magnetic behaviors in the sample with $y=0.2$ in this work. The higher magnetization for the sample with $y=0.1$ compared to the three remaining samples is probably caused by a small amount of α-Fe not detected by x-ray diffraction.

Figures 2(a) and 2(b) show some typical ZFC and FC $M(T)$ curves for the sample with $y=0.2$, respectively. As shown in Fig. 2(a), when $\mu_0H\geqslant 0.4$ T, the cusp observed around 70 K under 0.01 T suddenly transforms into a plateaulike anomaly, revealing the mixture of AFM state with

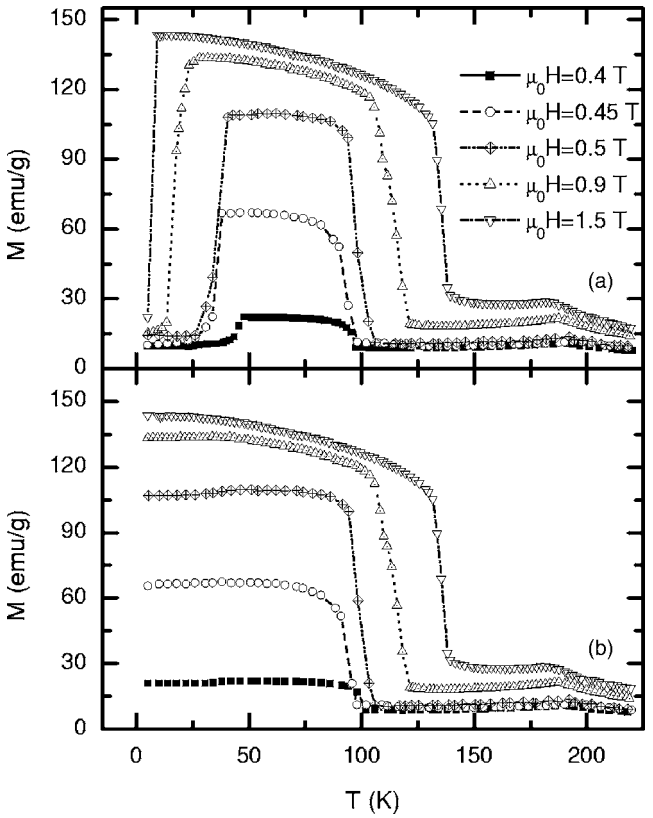

FIG. 2. (a) ZFC and (b) FC isofield magnetization curves for $Pr_{0.2}La_{0.8}Fe_{11.4}Al_{1.6}$ compound.

FM state. The magnitude of the plateaulike anomaly increases rapidly when the field rises up to 0.75 T, and slowly after that. Finally, the magnitude is nearly unchanged as $\mu_0H\geqslant 1.0$ T. On the other hand, the plateaulike region broadens gradually with the field increase. The feature of FC $M(T)$ curves as shown in Fig. 2(b) differs significantly from that of ZFC ones. The ZFC and FC $M(T)$ curves nearly superpose at high temperature, while the FC $M(T)$ curves deviate from the corresponding ZFC branches at low temperature.

As displayed in Fig. 3, T-H magnetic phase diagram for $Pr_{0.2}La_{0.8}Fe_{11.4}Al_{1.6}$ is constructed based on ZFC isofield magnetization curves. The transition between AFM and FM state is of the first order. The temperature difference between the transition starting and ending is ~15 K, as shown in Fig. 2. Here, for simplicity, the temperature where the derivative $\partial M/\partial T$ shows the maximum is used as the transition temperature. The low-temperature and high-temperature AFM states are labeled as AFMI and AFMII, respectively, only for convenience. Up to now, it is difficult for us to conclude whether AFMI is substantially equal to AFMII. As shown in Fig. 3, the temperature of AFMI-to-FM transition decreases with the increase of field, which is contrary to the case for AFMII-to-FM transition. Under the field of 5 T, no AFM state is observed, and the temperature of transition from FM to PM state is about 180 K according to the $M(T)$ curve.

Figure 4 exhibits some typical ZFC isothermal magnetization $M(H)$ curves for the $Pr_{0.2}La_{0.8}Fe_{11.4}Al_{1.6}$ compound. At 72 K, the magnetization almost follows the demagnetization path during the second field increase. Below 70 K, the

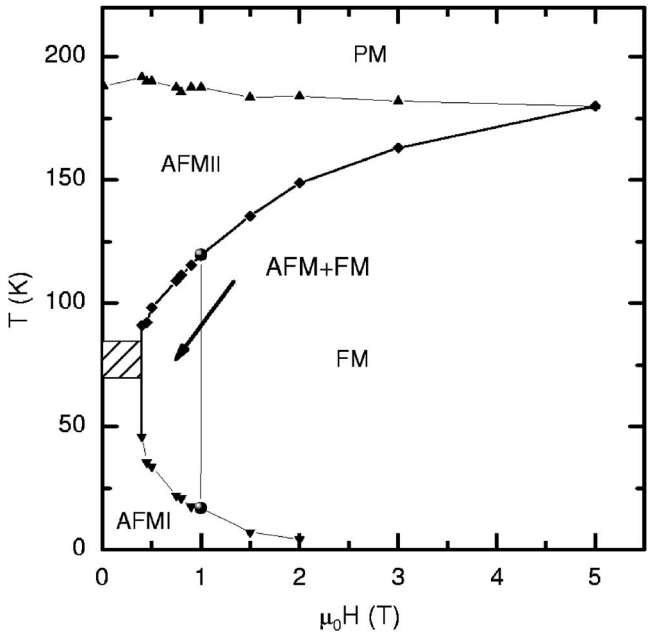

FIG. 3. ZFC magnetic phase diagram for $Pr_{0.2}La_{0.8}Fe_{11.4}Al_{1.6}$ compound.

second ascending-field curve fully superposes the descending-field one, indicating that $Pr_{0.2}La_{0.8}Fe_{11.4}Al_{1.6}$ remains in the ferromagnetic state upon removal of the field. In other words, the AFMI-to-FM transition is irreversible. On the contrary, at 83 K, the second ascending-field magnetization almost follows the initial magnetization path, and superposes the latter above 85 K, indicating a reversible AFMII-to-FM transition. At the temperature ranging from 70 to 85 K, the transition is partially reversible, as shown in Fig. 4. The partial reversibility of the transition under a low field is illustrated by the shadowed area in Fig. 3.

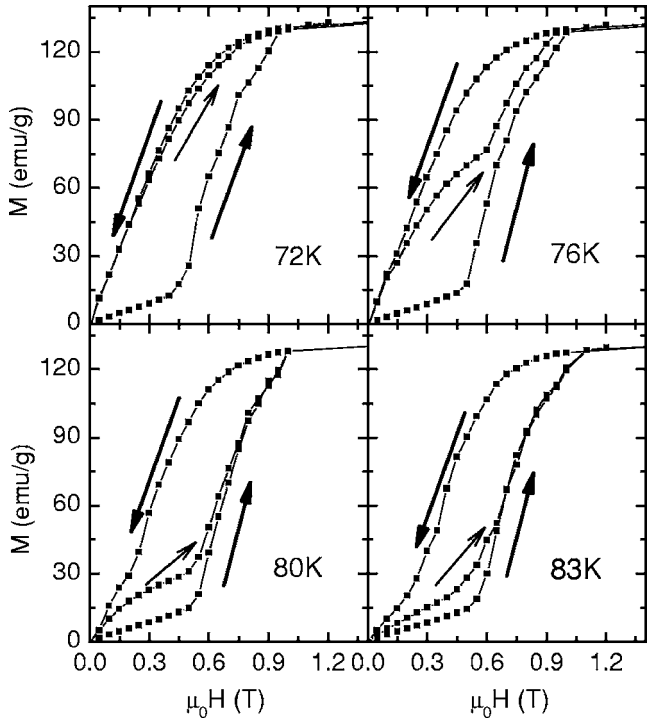

FIG. 4. ZFC isothermal magnetization curves for $Pr_{0.2}La_{0.8}Fe_{11.4}Al_{1.6}$ compound at 72, 76, 80, and 83 K. The thin arrow indicates the second ascending-field curve.

The above mentioned peculiar magnetic behaviors are similar to those observed in Gd_5Ge_4 (Refs. 12–16) and $LaFe_{11.4}Al_{1.6}C_{0.02}$ (Ref. 17) compounds. In Gd_5Ge_4, the AFM-to-FM transition is accompanied by a crystal structure transformation from the Sm_5Ge_4-type to the Gd_5Si_4-type structure, and shows a martensiticlike character. Furthermore, there is still argument about the low-temperature low-field region in the magnetic phase diagram. For example, in Ref. 14, this region is believed to be AFM, but the low-temperature AFM state is different from the high-temperature AFM state; in Ref. 15, the low-temperature AFM state is the same as the high-temperature one; in Ref. 16, this region is interestingly a magnetic glass state. Unlike the Gd_5Ge_4 compound, both $Pr_{0.2}La_{0.8}Fe_{11.4}Al_{1.6}$ and $LaFe_{11.4}Al_{1.6}C_{0.02}$ belong to a typical itinerant-electron system, and their itinerant-electron metamagnetic transition (IEMT) is characterized by the double minima of the states in the magnetic free energy as a function of magnetization.[18–20] Here, we give a phenomenological explanation for the peculiar magnetic phase diagram in both $Pr_{0.2}La_{0.8}Fe_{11.4}Al_{1.6}$ and $LaFe_{11.4}Al_{1.6}C_{0.02}$ compounds. The model is based on a combination of itinerant electronic metamagnetism and the theory for thermal activation. Most importantly, the model may be helpful in explaining the similar phenomena in other compounds, e.g., Gd_5Ge_4 compound.

The double free energy minima correspond to AFM and FM states in the $Pr_{0.2}La_{0.8}Fe_{11.4}Al_{1.6}$ compound. Here, $\Delta f_{\text{AFM-to-FM}}$ and $\Delta f_{\text{FM-to-AFM}}$ are defined as the energy barriers for the transitions from AFM to FM state and from FM to AFM state, respectively. Both $\Delta f_{\text{AFM-to-FM}}$ and $\Delta f_{\text{FM-to-AFM}}$ are the functions of temperature and field, i.e., $\Delta f_{\text{AFM-to-FM}}(T,H)$ and $\Delta f_{\text{FM-to-AFM}}(T,H)$.[18–20] With the increase of field, $\Delta f_{\text{AFM-to-FM}}$ decreases, while $\Delta f_{\text{FM-to-AFM}}$ increases. If $\Delta f_{\text{AFM-to-FM}}$ is less (or larger) than $\Delta f_{\text{FM-to-AFM}}$, the FM (or AFM) state is stable. But, AFM state can exist metastably as $\Delta f_{\text{AFM-to-FM}} > \Delta f_{\text{FM-to-AFM}} > 0$. In this case, the appearance of AFM or FM state depends on the history of field and/or temperature variation. For the $Pr_{0.2}La_{0.8}Fe_{11.4}Al_{1.6}$ compound, as shown in Fig. 4, the AFM state is stable above 85 K, indicative of $\Delta f_{\text{AFM-to-FM}} > \Delta f_{\text{FM-to-AFM}}$. AFM state becomes metastable below 70 K, suggesting $\Delta f_{\text{AFM-to-FM}} > \Delta f_{\text{AFM-to-FM}} > 0$. The observation of a metastable AFM state at low temperature results from the fact that the sample is cooled from room temperature.

For a given temperature and a given field, the IEMT may happen by thermal activation when $\Delta f_{\text{AFM-to-FM}}$ (or $\Delta f_{\text{FM-to-AFM}}$) is comparable with the thermal energy $k_B T$.[21] Before a barrier Δf (i.e., $\Delta f_{\text{AFM-to-FM}}$ or $\Delta f_{\text{FM-to-AFM}}$) is overcome, the mean waiting time τ is given by $\tau = \tau_0 \exp(\Delta f / k_B T)$ for thermal activation, where τ_0 is a constant of order 10^{-10}–10^{-12} s.[22] In this work, τ_0 is taken as $\exp(-25)$. So, τ is 1 s and about 1000 s for $\Delta f = 25 k_B T$ and $32 k_B T$, respectively. Within the time scale of an experiment, it is usually considered that a transition with $\tau \leqslant 1$ s has finished, and one with $\tau > 1000$ s has not happened. For simplicity, we define $\tau = 1$ and 1000 s, corresponding to the energy barriers of $25 k_B T$ and $32 k_B T$,[22] as the ending and

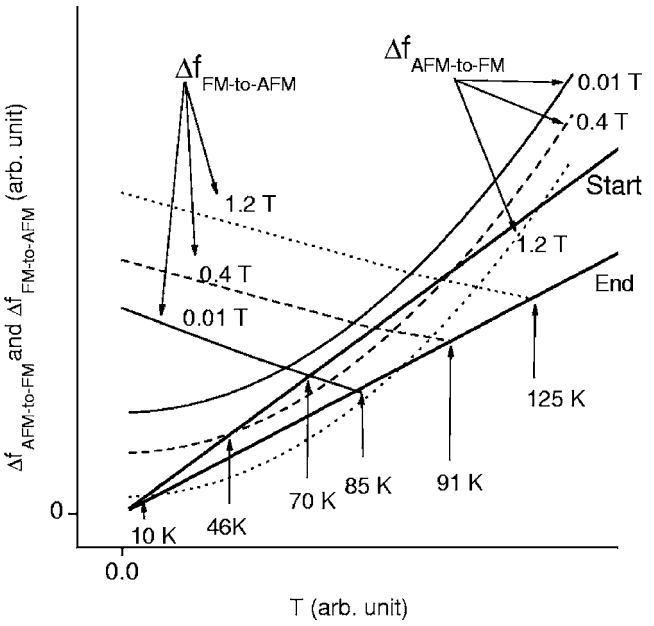

FIG. 5. The variation of $\Delta f_{\text{AFM-to-FM}}$ and $\Delta f_{\text{FM-to-AFM}}$ with temperature. Here, the solid, dashed, and dotted curves are the representative of the case for $\mu_0 H=0.01$, 0.4, and 1.2 T, respectively. The thick lines with small and large slopes represent the energy barriers of $25k_BT$ and $32k_BT$, respectively.

starting times of the phase transition, respectively. Therefore, according to the phase diagram (shown in Fig. 3) and the reversibility of the transition (as shown in Fig. 4), we suppose that the sketch map of the $\Delta f_{\text{AFM-to-FM}}$ and $\Delta f_{\text{FM-to-AFM}}$ varies with temperature and field as shown in Fig. 5.

According to the sketch map shown in Fig. 5, the AFM state remains metastably at low temperature after a zero-field cooling, consistent with the experimental results. By warming up the sample under 0.01 T (see the solid line for $\Delta f_{\text{AFM-to-FM}}$ in Fig. 5), the cusp broadens around 70 K in the $M(T)$ curve (shown in Fig. 1) due to $\Delta f_{\text{AFM-to-FM}}$ very close to $32k_BT$. When the field of 0.4 T is switched on after a ZFC process (see the dash line for $\Delta f_{\text{AFM-to-FM}}$ in Fig. 5), the AFM state partially changes to a FM state as T increases up to 46 K because of $25k_BT<\Delta f_{\text{AFM-to-FM}}<32k_BT$. It is noted that the reduced FM state follows the dash line for $\Delta f_{\text{FM-to-AFM}}$ rather than that for $\Delta f_{\text{AFM-to-FM}}$ to evolve into an AFM state. Further increasing the temperature up to 91 K, the induced FM state becomes unstable because of $\Delta f_{\text{FM-to-AFM}}<25k_BT$ (see the dash line for $\Delta f_{\text{FM-to-AFM}}$). On the other hand, when the sample is cooled from 200 K under 0.4 T, a FM state is partially induced at $T<91$ K (see the dash line for $\Delta f_{\text{AFM-to-FM}}$ in Fig. 5) because of $25k_BT<\Delta f_{\text{AFM-to-FM}}<32k_BT$. Thus, the measured state at 5 K is the mixture of AFM state with FM state, which results in the divergence of FC branch from ZFC one (as shown in Fig. 2). The induced FM state cannot jump back to the AFM state due to $\Delta f_{\text{FM-to-AFM}}>32k_BT$ (see the dash line for $\Delta f_{\text{FM-to-AFM}}$) until the sample is warmed up to about 85 K. By further warming up the sample to the temperature higher than 91 K, the induced FM state fully changes to an AFM state due to $\Delta f_{\text{FM-to-AFM}}<25k_BT$. When the sample is cooled under 1.2 T, the AFM state will disappear as soon as $\Delta f_{\text{AFM-to-FM}}<25k_BT$ (see the dot line for $\Delta f_{\text{AFM-to-FM}}$ in Fig. 5). In this case, the magnetic state at low temperature becomes purely FM. The reentrance of an AFM state takes place only when the sample is warmed up to 125 K, i.e., $\Delta f_{\text{FM-to-AFM}}<25k_BT$.

Now, let us probe into the case of $M(H)$. As shown in Fig. 5, at a given temperature less than 70 K, the AFM phase completely disappears when $\Delta f_{\text{AFM-to-FM}}<25k_BT$ is satisfied by increasing the field. Subsequently, the FM state remains even under zero field because of $\Delta f_{\text{FM-to-AFM}}>32k_BT$. Above 85 K, the reversibility of the AFMII-to-FM transition is caused by $\Delta f_{\text{FM-to-AFM}}<25k_BT$ under zero field. In the temperature range between 70 and 85 K, $32k_BT>\Delta f_{\text{FM-to-AFM}}>25k_BT$ results in the partially reversible transition as shown in Fig. 4. Thus, based on the sketch map as shown in Fig. 5, the peculiar magnetic properties have been well explained at least qualitatively. The validity of the sketch map needs to be further verified using the electronic structure information, because $\Delta f_{\text{AFM-to-FM}}$ and $\Delta f_{\text{FM-to-AFM}}$ are both determined by the density of states near the Fermi level.

ACKNOWLEDGMENTS

The work was supported by the State Key Project of Fundamental Research and the National Natural Science Foundation of China.

[1] T. T. M. Palstra, G. J. Nieuwenhuys, J. A. Mydosh, and K. H. J. Buschow, J. Appl. Phys. **55**, 2367 (1984).
[2] T. T. M. Palstra, G. J. Nieuwenhuys, J. A. Mydosh, and K. H. J. Buschow, Phys. Rev. B **31**, 4622 (1985).
[3] T. T. M. Palstra, H. G. C. Werij, G. J. Nieuwenhuys, J. A. Mydosh, F. R. de Boer, and K. H. J. Buschow, J. Phys. F: Met. Phys. **14**, 1961 (1984).
[4] M. M. Abd-Elmeguid, B. Schleede, H. Micklitz, T. T. M. Palstra, G. J. Nieuwenhuys, and K. H. J. Buschow, Solid State Commun. **63**, 177 (1987).
[5] K. Irisawa, A. Fujita, and K. Fukamichi, J. Alloys Compd. **305**, 17 (2000).
[6] O. Moze, W. Kockelmann, J. P. Liu, F. R. de Boer, and K. H. J. Buschow, J. Magn. Magn. Mater. **195**, 391 (1999).
[7] K. Irisawa, A. Fujita, K. Fukamichi, Y. Yamazaki, Y. Iijima, and E. Matsubara, J. Alloys Compd. **316**, 70 (2001).
[8] F. Wang, Y. F. Chen, G. J. Wang, J. R. Sun, and B. G. Shen, J. Phys.: Condens. Matter **16**, 2103 (2004).
[9] K. Irisawa, A. Fujita, K. Fukamichi, M. Yamada, H. Mitamura, T. Goto, and K. Koyama, Phys. Rev. B **70**, 214405 (2004).
[10] X. B. Liu, Z. Altounian, and D. H. Ryan, J. Phys. D **37**, 2469 (2004).
[11] R. B. Helmholdt, T. T. M. Palstra, G. J. Nieuwenhuys, J. A. Mydosh, A. M. van der Kraan, and K. H. J. Buschow, Phys. Rev. B **34**, 169 (1986).
[12] E. M. Levin, K. A. Gschneidner, Jr., and V. K. Pecharsky, Phys. Rev. B **65**, 214427 (2002).
[13] V. K. Pecharsky, A. P. Holm, K. A. Gschneidner, and R. Rink, Phys. Rev. Lett. **91**, 197204 (2003).
[14] H. Tang, V. K. Pecharsky, K. A. Gschneidner, Jr., and A. O. Pecharsky, Phys. Rev. B **69**, 064410 (2004).
[15] Y. Mudryk, A. P. Holm, K. A. Gschneidner, and V. K. Pecharsky, Phys. Rev. B **72**, 064442 (2005).
[16] S. B. Roy, M. K. Chattopadhyay, P. Chaddah, J. D. Moore, G. K. Perkins, L. F. Cohen, K. A. Gschneidner, and V. K. Pecharsky, Phys. Rev. B **74**, 012403 (2006).
[17] H. W. Zhang, J. Chen, G. J. Liu, L. G. Zhang, J. R. Sun, and B. G. Shen, Phys. Rev. B **74**, 212408 (2006).
[18] E. P. Wohlfarth and P. Rhodes, Philos. Mag. **7**, 1817 (1962).
[19] M. Shimizu, J. Phys. (Paris) **43**, 155 (1982).
[20] R. Z. Levitin and A. S. Markosyan, Sov. Phys. Usp. **31**, 730 (1988).
[21] H. W. Zhang, F. Wang, T. Y. Zhao, S. Y. Zhang, J. R. Sun, and B. G. Shen, Phys. Rev. B **70**, 212402 (2004).
[22] P. Gaunt, Philos. Mag. **34**, 775 (1976).